Global sensitivity of high-resolution estimates of crop water footprint

AGU PUBLICATIONS

Water Resources Research

RESEARCH ARTICLE
10.1002/2015WR017148

Key Points:
- The virtual water content of crops is highly variable in space
- VWC high-resolution maps are obtained with up-to-date data sets
- The VWC is most sensitive to agricultural practices than climate

Supporting Information:
- Supporting Information S1

Correspondence to:
M. Tuninetti,
marta.tuninetti@polito.it

Citation:
Tuninetti, M., S. Tamea, P. D'Odorico, F. Laio, and L. Ridolfi (2015), Global sensitivity of high-resolution estimates of crop water footprint, *Water Resour. Res.*, *51*, 8257–8272, doi:10.1002/2015WR017148.

Received 26 FEB 2015
Accepted 16 SEP 2015
Accepted article online 21 SEP 2015
Published online 17 OCT 2015

Global sensitivity of high-resolution estimates of crop water footprint

Marta Tuninetti[1], Stefania Tamea[1], Paolo D'Odorico[2], Francesco Laio[1], and Luca Ridolfi[1]

[1]Department of Environmental, Land, and Infrastructure Engineering, Politecnico di Torino-24, Corso Duca degli Abruzzi, Torino, Italy, [2]Department of Environmental Sciences, University of Virginia, Charlottesville, Virginia, USA

Abstract Most of the human appropriation of freshwater resources is for agriculture. Water availability is a major constraint to mankind's ability to produce food. The notion of virtual water content (*VWC*), also known as crop water footprint, provides an effective tool to investigate the linkage between food and water resources as a function of climate, soil, and agricultural practices. The spatial variability in the virtual water content of crops is here explored, disentangling its dependency on climate and crop yields and assessing the sensitivity of *VWC* estimates to parameter variability and uncertainty. Here we calculate the virtual water content of four staple crops (i.e., wheat, rice, maize, and soybean) for the entire world developing a high-resolution (5×5 arc min) model, and we evaluate the *VWC* sensitivity to input parameters. We find that food production almost entirely depends on green water (>90%), but, when applied, irrigation makes crop production more water efficient, thus requiring less water. The spatial variability of the *VWC* is mostly controlled by the spatial patterns of crop yields with an average correlation coefficient of 0.83. The results of the sensitivity analysis show that wheat is most sensitive to the length of the growing period, rice to reference evapotranspiration, maize and soybean to the crop planting date. The *VWC* sensitivity varies not only among crops, but also across the harvested areas of the world, even at the subnational scale.

1. Introduction

Water consumption for food production is by far the biggest form of societal use of water [*Falkenmark and Rockström*, 2004] with irrigation accounting for about 70% of the total freshwater withdrawals for human uses [*FAO*, 2011]. In a world with continuously rising demographic pressure and changing diets, water availability is becoming increasingly crucial for food security and human welfare [*Godfray et al.*, 2010; *Tilman et al.*, 2011]. The world population of 7.2 billion in early 2015 is projected to increase to 9.6 billion in 2050 [*United Nations, Department of Economic and Social Affairs, Population Division*, 2013], resulting in a 70% increase in the global demand for agricultural products [*FAO*, 2011], with irrigated agriculture playing a strategic role. Climate change is expected to worsen this picture by increasing the spatial heterogeneity of water resource availability [*FAO*, 2011]. Presently, some regions of the world already exhibit major depletion of freshwater resources due to withdrawals for agriculture [*Gleick*, 2000; *Wada et al.*, 2010]. Scientists, policy makers, and the general public are realizing that meeting the competing water needs of ecosystems and societies is a major environmental challenge for this century [*Dudgeon et al.*, 2006; *Hanjra and Qureshi*, 2010]. Thus, understanding the food-water nexus is crucial to the global environmental change debate and the design of strategies for sustainable development [*Fedoroff et al.*, 2010].

The notion of virtual water content (*VWC*) provides an effective tool to investigate the linkage between food and water resources [*Antonelli and Sartori*, 2015]. The virtual water content is defined as the amount of water needed to produce a given food commodity [*Allan*, 2003]; therefore, it represents the amount of water that is conceptually embedded (though not physically present) in a good. The concept of *VWC* allows for a comparison of different commodities on the basis of their water cost. Moreover, the virtual water content can be quantified in terms of a green and a blue water component, depending on whether the water is contributed by precipitation water stored in the (top of) soil and vegetation, or by surface and groundwater used for irrigation and food processing. Therefore in this context, with these specifications, the notions of virtual water content and crop water footprint can be used interchangeably [*Hoekstra and Chapagain*, 2011].

A growing number of studies has used the virtual water concept for a variety of purposes, ranging from the global analysis of the virtual water trade [e.g., *Konar et al.*, 2011; *Carr et al.*, 2013; *Tamea et al.*, 2014] to water

Table 1. Studies About the Global *VWC* of Crop Production at High Spatial Resolution Scale

Study	Scale	Resolution	Period	Crop Yield	Rainfall	ET0	Soil	Sensitivity
Rost et al. [2008]	Global	0.5 deg	1971–2000		0.5 deg	0.5 deg	0.5 deg	No
Hanasaki et al. [2010]	Global	0.5 deg	1985–1999	Country	1 deg	1 deg	Uniform	No
Liu and Yang [2010]	Global	0.5 deg	2000		0.5 deg	0.5 deg	5 arc min	No
Siebert and Döll [2010]	Global	5 arc min	1998–2002	5 arc min	10 arc min	10 arc min	5 arc min	No
Mekonnen and Hoekstra [2011]	Global	5 arc min	1996–2005	5 arc min	0.5 deg	10 arc min	5 arc min	No
Zhuo et al. [2014]	Local	5 arc min	1996–2005	5 arc min	0.5 deg	10 arc min	5 arc min	Yes
This study	Global	5 arc min	1996–2005	5 arc min	10 arc min	10 arc min	0.5 arc min	Yes

sustainability studies [e.g., *Seekell et al.*, 2011; *Wichelns*, 2004] and water use accounting [e.g., *Hoekstra and Hung*, 2002; *Chapagain and Hoekstra*, 2004; *Kummu et al.*, 2012; *Vanham et al.*, 2013]. The above studies deal with either the entire world, or with continents or single countries. In recent years, there have been various attempts to assess global water use for crop production at higher spatial resolution. Table 1 summarizes the main features of higher-resolution studies on the global *VWC* assessment. *Rost et al.* [2008] mapped (with a spatial resolution of 0.5 × 0.5 arc deg resolution) the total consumption of green and blue water by rainfed and irrigated agriculture for 12 crops and 9 plant functional types, for a reference period 1971–2000. *Hanasaki et al.* [2010] reported the global green and blue water consumption for five crops and three livestock products at 0.5 × 0.5 arc deg resolution, along the period 1985–1999. *Liu and Yang* [2010] made a global estimate of green and blue water consumption for crop production at 0.5 arc deg resolution. *Siebert and Döll* [2010] quantified the green and blue virtual water contents of 26 crops with a spatial resolution of 5 × 5 arc min in the period 1998–2002. In a recent study, *Mekonnen and Hoekstra* [2011] estimated the green, blue, and gray water footprints of 126 crops with a spatial resolution of 5 × 5 arc min, relatively to the period 1996–2005. All these studies depend on a large set of assumptions with respect to modeling structure, input parameters, and data sets used. Only very few studies, however, have developed a sensitivity analysis of the water footprint calculations to define the accuracy of the final outcomes. Their focus has been on specific regions, such as the Yellow River basin in China [*Zhuo et al.*, 2014] and the Po valley in Northern Italy [*Bocchiola et al.*, 2013]. To date, a global-scale sensitivity analysis with high spatial resolution is still missing.

In the present study, we investigate the water footprint of major crops and their spatial variability at a subnational scale. To this end, we produce 5 × 5 arc min resolution maps of the virtual water content of the main cultivated grains using new high-resolution spatial data recently available for precipitation, evapotranspiration, agricultural yields, and soil water content. We use for the first time in a *VWC* assessment (to the best of our knowledge) the 30 arc sec maps of soil water available content given by *FAO/IIASA/ISRIC/ISSCAS/JRC* [2012] and the 10 arc min maps of monthly precipitation given by *New et al.* [2002] (see Table 1). Moreover, unlike previous high spatial resolution studies, we account for the existence of multiple growing seasons as in *Siebert and Döll* [2010]. We analyze the spatial heterogeneity of the *VWC* both at the grid-cell scale, to evaluate whether differences in virtual water content are more determined by potential evapotranspiration patterns or by yield differences, but also at the continental scale, to investigate the relationship existing between *VWC* and commodity production. We also study the sensitivity of crop water footprint to climate and soil parameters and evaluate how the unavoidable uncertainties existing in the (spatial) climate and soil data affect the calculation of the virtual water content of crops (hence, informing future efforts aiming at the refinement of data used in the assessment of agricultural water requirements). The results of this study lend themselves to the identification of the parameters (e.g., duration of the growing season, planting date, etc.) that farmers and land managers can modify to more effectively reduce the water cost of crop production.

We focus on the four most cultivated grains, namely, wheat, rice, maize, and soybean, which account for more than 50% of the global human diet in terms of caloric content (wheat: 20%, rice: 16%, maize: 13%, and soybean: 8%) [*D'Odorico et al.*, 2014], and more than 50% of the global crop water footprint [*Mekonnen and Hoekstra*, 2011].

2. Data and Methods

2.1. Evaluation of Crop Virtual Water Content

The virtual water content of crops is evaluated globally at the spatial resolution of 5 × 5 arc min, corresponding to pixels of about 9 km × 9 km at the equator. We consider both rainfed and irrigated production

conditions, as well as multicropping practices (i.e., a crop can be grown on the same land more than once a year). *VWC* estimates are referred to the time interval from 1996 to 2005. We chose a data range of 10 years in order to have input data independent of interannual fluctuations and typical of each grid cell; more specifically, we build our reference period centered on year 2000 because this is the most frequent reference year in the global agricultural data sets used in this study (e.g., crop calendar, crop yields, and harvested areas).

Virtual water content, *VWC*, is defined in each pixel as the ratio between the water evapotranspired by the crop during the growing seasons of a year *y*, $ET_{a,y}$ (mm), and the crop actual yield, Y_a (ton ha^{-1}), as

$$VWC = \frac{10 \cdot ET_{a,y}}{Y_a} \qquad \left(\frac{\mathrm{m}^3}{\mathrm{ton}}\right), \tag{1}$$

where the factor 10 converts the evapotranspired water height expressed in mm into a water volume per land surface expressed in m^3 ha^{-1}.

In regions where more than one crop per year is planted and harvested (i.e., there are multiple growing seasons), the actual evapotranspiration of a year, $ET_{a,y}$, is calculated as the weighted average (with respect to the area A_n cultivated during the growing period n with $n = 1, 2, \ldots$) of the total actual evapotranspiration $ET_{a,LPG,n}$ (mm) of each growing season, as

$$ET_{a,y} = \frac{\sum_n (ET_{a,LGP,n} \cdot A_n)}{\sum_n A_n} \qquad (\mathrm{mm}), \tag{2}$$

where *LGP* is the length of each growing period. Depending on agricultural practices, climate and soil properties, the crop evapotranspires green ($ET_{g,y}$) and/or blue water ($ET_{b,y}$). Thus, the total water evapotranspired by the crop during the growing seasons of a year can be written as the sum of a green and a blue component,

$$ET_{a,y} = ET_{g,y} + ET_{b,y}. \tag{3}$$

2.1.1. Crop Evapotranspiration Over a Single Growing Season

The total water evapotranspired by the crop in a single growing season, $ET_{a,LGP}$ (mm), is obtained by summing up over the length of the growing period (*LGP*) the daily actual evapotranspiration, $ET_{a,j}$ (mm d^{-1}), i.e.,

$$ET_{a,LGP} = \sum_{j=1}^{LGP} ET_{a,j} \qquad (\mathrm{mm}), \tag{4}$$

with *j* indicating the day of the growing period. *LGP* is delimited by the planting (*PD*) and harvesting dates taken from *Portmann et al.* [2010]. This data set distinguishes between rainfed and irrigated production and provides the month in which the growing period starts and ends at 5 × 5 arc min resolution, considering multicropping practices, for year 2000. We initially assume that the cropping period starts and ends in the middle of the month.

Daily crop evapotranspiration, $ET_{a,j}$, is calculated following *Allen et al.* [1998], a well-established approach for the virtual water content assessment [*Mekonnen and Hoekstra*, 2011; *Siebert and Döll*, 2010; *Zhuo et al.*, 2014]. $ET_{a,j}$ is defined as

$$ET_{a,j} = k_{c,j} \cdot ET_{0,j} \cdot k_{s,j} \qquad \left(\frac{\mathrm{mm}}{\mathrm{d}}\right), \tag{5}$$

where $k_{c,j}$ is the daily crop coefficient, $ET_{0,j}$ is the daily reference evapotranspiration (mm d^{-1}) from a hypothetical well-watered grass surface with fixed crop height, albedo and canopy resistance, and $k_{s,j}$ is the daily water stress coefficient depending on the available soil water content, with a value between 0 (maximum water stress) and 1 (no water stress).

The crop coefficient, $k_{c,j}$, depends on crop characteristics and, to a limited extent, on climate. It is influenced by crop height, albedo, canopy resistance, and evaporation from bare soil. During the growing period, $k_{c,j}$

varies with a characteristic shape divided into four growing stages (I: initial phase, II: development stage, III: midseason, and IV: late season) of l_I, l_{II}, l_{III}, and l_{IV} days length, respectively, that reads

$$k_{c,j}=\begin{cases} k_{c,in} & \text{j} \in \text{I stage} \\ j \cdot \dfrac{k_{c,mid}-k_{c,in}}{j-l_I} & \text{j} \in \text{II stage} \\ k_{c,mid} & \text{j} \in \text{III stage} \\ j \cdot \dfrac{k_{c,f}-k_{c,mid}}{j-l_I-l_{II}-l_{III}} & \text{j} \in \text{IV stage.} \end{cases} \quad (6)$$

We use values from *Allen et al.* [1998] for the constants $k_{c,in}$, $k_{c,mid}$, $k_{c,f}$, while the length of each stage, l_{st}, is calculated as a fraction, p_{st}, of the length of the growing period ($l_{st}=p_{st} \cdot LGP$); p_{st} is defined for each stage (with $st=I-IV$) according to *Mekonnen and Hoekstra* [2011], whose study provides specific values of p_{st} for different climatic regions. Lengths are rounded to the nearest integer and the stage I is adjusted to guarantee the exact length of the growing period.

Monthly long-term average reference evapotranspiration data, $ET_{0,m}$, at 10 × 10 arc min resolution are given by *FAO* [2014]. These data are converted to 5 × 5 arc min data by subdividing each grid cell into four square elements and assigning them the correspondent 10 × 10 values. Daily $ET_{0,j}$ values are determined through a linear interpolation of monthly climatic data and attributing the monthly $ET_{0,m}$ value to the middle of the month. For sake of simplicity, we consider months 30 days long. These conversions introduce uncertainties in the calculation of the *VWC*, but they are necessary because of the lack of daily evapotranspiration data at 5 × 5 arc min resolution.

The water stress coefficient typical of the cell, $k_{s,j}$, varies during the growing period depending on the total available water content (*TAW*) and the readily available water content (*RAW*) in the root zone [*Allen et al.*, 1998]. The water stress coefficient is evaluated considering two different types of production: rainfed production (*R*), in which crops are fed only by precipitation, and irrigated production (*I*), in which crops are irrigated when necessary in order to prevent the emergence of water stress. In the irrigated production the water stress coefficient, $k_{s,j}$, is equal to 1 throughout the growth period. In the rainfed production, the computation of the $k_{s,j}$ daily value is detailed in Appendix A. In its evaluation, we use for the first time in a *VWC* assessment (to the best of our knowledge) the 30 arc sec maps of the available water content (*AWC*) given by *FAO/IIASA/ISRIC/ISSCAS/JRC* [2012] and the 10 arc min maps of monthly precipitation given by *New et al.* [2002]. Since the daily $k_{s,j}$ is different in the two production types (rainfed versus irrigated), as well as the $ET_{0,j}$ (i.e., the growing period can have different planting dates in rainfed and irrigated conditions), the daily actual evapotranspiration (green + blue), $ET_{a,j}$, calculated with equation (5), is different in the two production types. The green component for rainfed crops, $ET^R_{g,j}$, is equal to the total evapotranspiration, $ET^R_{a,j}$. The blue component for irrigated crops, $ET^I_{b,j}$ (notice that by definition, $ET^R_{b,j}=0$), is obtained as the amount of irrigation water provided to the crop; the green component is the difference between the $ET^I_{a,j}$ and $ET^I_{b,j}$ values. The total, green and blue evapotranspiration over the growing period are given by equation (4), both for rainfed ($ET^R_{g,LGP}$) and irrigated conditions ($ET^I_{g,LGP}$ and $ET^I_{b,LGP}$).

The overall evapotranspiration of green and blue water from the cell, $ET_{g,LGP}$ and $ET_{b,LGP}$, is the weighted mean of the rainfed and irrigated evapotranspiration,

$$ET_{g,LGP}=\frac{ET^R_{g,LGP} \cdot A^R+ET^I_{g,LGP} \cdot A^I}{A^R+A^I}, \quad (7)$$

$$ET_{b,LGP}=\frac{ET^I_{b,LGP} \cdot A^I}{A^R+A^I}, \quad (8)$$

where weights, A^R and A^I, are the harvested areas given by *Portmann et al.* [2010]. This data set distinguishes rainfed and irrigated production, providing the harvested areas of 26 main crops, for each growing season. The procedure to evaluate the values of $ET_{g,LGP}$ and $ET_{b,LGP}$ is repeated for each growing season of a year; equation (2) is then applied to determine the green and blue evapotranspiration of a year.

Due to peculiarities of the rice cultivation, the *VWC* estimates need further details. Rice is typically cultivated in wetland or upland systems. About 85% of the rice in the world is grown in wetland systems and about

75% of rice production is obtained from irrigated sites [*Bouman et al*., 2007]. In wetland rice cultivations, paddy fields are prepared and the soil is kept saturated. Basically, in the month before sowing or transplanting, water is used to saturate the root zone and the amount of water needed depends on the soil type and rooting depth, we considered a volume per unit area of 200 mm, as suggested by *Bouman et al*. [2007]. Moreover, during the growing season a constant percolation of water occurs below the root zone, whose rate is affected by a number of soil factors [*Wickham and Singh*, 1978]. In this study, we assume a 2.5 mm d^{-1} flux, corresponding to rather impermeable soils with a clayey texture [*Chapagain and Hoekstra*, 2011].

2.1.2. Crop Actual Yield

Subnational data sets of crop yields at high spatial resolution are seldom available. *Monfreda et al*. [2008] and the FAOSTAT database provide good estimates of yield values. The first one refers to year 2000 providing the observed yields and harvested areas of 175 distinct crops on a 5 × 5 arc min grid. This data set has been widely used both for the *VWC* assessment [e.g., *Siebert and Döll*, 2010; *Hanasaki et al*., 2010] and in analyses on crop yield-gaps [e.g., *Lobell et al*., 2009; *Mueller et al*., 2012]. The FAOSTAT database provides annual yields at the country scale from year 1961 to 2013. In order to obtain high-resolution actual yields, $Y_{a,T}$, referred to the investigated period, $T=[1996, 2005]$, we use the above mentioned data sources combined in the following relationship as:

$$Y_{a,T}(i,T)=g(i,2000)\cdot f(c,T), \tag{9}$$

where $g(i,2000)$ defines the ratio of cell yield to country yield for year 2000 (i is the cell of the grid), and $f(c, T)$ describes the country-scale (c indicates the country) yield in the investigated interval T. More specifically, $g(i,2000)$ is defined in each cell as

$$g(i,2000)=\frac{Y_a(i,2000)}{Y_a(c,2000)} \quad [—], \tag{10}$$

where $Y_a(i,2000)$ is the yield measured in the cell in year 2000 (given by *Monfreda et al*. [2008]), and $Y_a(c, 2000)$ is the country-based yield in the cell for the same year (given by FAOSTAT). The function $f(c, T)$ is the average of the national yields given by FAOSTAT for each year t of the study period, T, namely $f(c,T)=1/10\cdot\sum_{t=1996}^{t=2005} Y_a(c,t)$.

Finally, the green and blue *VWC* in each grid cell are determined with equation (1), substituting $ET_{a,y}$ with $ET_{g,y}$ for the green component and with $ET_{b,y}$ for the blue component *VWC*. The total virtual water content of the cell is the sum of the green and blue content (equation (3)).

2.2. Sensitivity Analysis

A sensitivity analysis is required to understand how data uncertainty propagates through the virtual water content estimates and to identify the model inputs that significantly affect the model outputs. To this aim, a first-order sensitivity analysis is applied: the functional dependence of *VWC* on each input parameter is expanded as a Taylor series and truncated at the first order; in this way a linear relationship between the *VWC* estimate and the generic input parameter, x, is assumed in a small neighborhood of x. Parameters are perturbed one-at-a-time of a very small quantity, which is arbitrarily chosen. To evaluate and compare the sensitivity of the *VWC* to different parameters, we define a normalized sensitivity index, SI_x, for each parameter, x, as

$$SI_x=\left(\frac{\Delta VWC}{VWC_0}\right)\Big/\left(\frac{\Delta x}{x_{ref}}\right), \tag{11}$$

where ΔVWC is the virtual water content variation resulting from changing the parameter x of a quantity Δx. Both variations are normalized: ΔVWC with respect to the virtual water content (VWC_0) estimated when all parameters are at their baseline values, while Δx with respect to a reference value of the parameter, x_{ref} (see Appendix B). Positive and negative variations of the input parameters are considered to analyze the response of the *VWC* both in terms of magnitude and direction of the change. The sensitivity analysis focuses on four key input parameters, namely monthly reference evapotranspiration ($ET_{0,m}$), available water content (*AWC*), planting date (*PD*), and length of the growing period (*LGP*). The reference evapotranspiration and the available water content are varied by ±0.01 mm d^{-1} and ±1 mm/m, respectively, while the planting date and the length of the growing are changed by ±1 day. The imposed variations are different from parameter to parameter, depending on their standard deviation, average, and range of variation. All

changes are lower than 2% of the standard deviation and lower than 1% of the range, in order to guarantee that variations are small.

For each single variation, the new *VWC* value is calculated. The *VWC* variation (ΔVWC) is due to a variation of the water volume evapotranspired by the crop during the growing season ($ET_{a,LGP}$) and to a variation of the crop actual yield (Y_a). The new evapotranspiration, $ET'_{a,LGP}$, is determined by the equations (4) and (5) where the modified parameter is introduced. The new yield, Y'_a (whose variation is affected by the evapotranspiration change), is determined through a modified expression of the equation by *Doorenbos and Kassam* [1979],

$$\left(1-\frac{Y'_a}{Y_a}\right)=K_y\cdot\left(1-\frac{ET'_{a,y}}{ET_{a,y}}\right), \tag{12}$$

where K_y is the yield response factor, representing the effect of a reduction in evapotranspiration on yield losses, Y_a and Y'_a are the actual yields before and after the input parameter change, respectively, and $ET_{a,y}$ and $ET'_{a,y}$ are the crop actual evapotranspiration before and after the change of the input parameter.

3. Results

In this section, we first analyze the high-resolution maps of the virtual water content of wheat, rice, maize, and soybean, focusing on the role of evapotranspiration and yield in determining the spatial distribution of *VWC*. In order to support and validate the results of this study, we make a comparison of our *VWC* estimates with those from previous studies. Second, we describe the *VWC* variability at a continental scale, showing the relation between virtual water content and commodity production.

3.1. High-Resolution Maps of Virtual Water Content

Figure 1 is an example of the high-resolution maps obtained in this study. It reports the spatial distribution of the total and blue virtual water content of wheat, typical of the period between 1996 and 2005. The maps show a strong spatial heterogeneity both inside the climatic regions and at the subnational scale. The observed spatial variability is mainly driven by the yield pattern with a correlation coefficient of 0.74, while the influence of the evapotranspiration demand (hence, climate), is lower with a correlation of 0.34. Looking at the maps, one can immediately notice the high water efficiency of the United States (especially on the West Coast), Europe, and China, where the virtual water content is generally lower than 2000 m^3 ton^{-1}, with a consumption of blue water less than 10% of the total water consumption in the United States and Europe, and between 50% and 75% in the large cropping area in the north-east of China. South America, Africa, and Southern Asia are less water efficient, with *VWC* reaching up to 6000–8000 m^3 ton^{-1} in some regions of Venezuela, Ethiopia, and Vietnam. Details about such a heterogeneous distribution are given in the supporting information, where yield gaps and crop evapotranspiration patterns are also described. In the supporting information, we also provide the spatial variability of the *VWC* for the other crops (namely, rice, maize, and soybean), through maps (supporting information Figures S1–S3), followed by a discussion.

The distributed results are aggregated at the country and global scale by a weighted mean (using cell production as weight) in order to make a comparison with the results from earlier studies. At national scale, our *VWC* estimates are in good agreement with those from *Hanasaki et al*. [2010], particularly for maize production, as can be seen in Table 2 for the major exporting countries. National *VWC* values estimated in the present work are also in close agreement with those from *Mekonnen and Hoekstra* [2011], as confirmed by the coefficients of determination, R^2_w, that are 0.91 for wheat, 0.76 for rice, 0.90 for maize, and 0.91 for soybean (R^2_w is weighted with the countries production). At global scale, *VWC* averages estimated in this study well compare with those from *Siebert and Döll* [2010] and *Mekonnen and Hoekstra* [2011], especially for wheat and maize production, as can be seen in Table 3.

3.2. Distribution of VWC Related to Production

We evaluated the distribution of *VWC* as a function of yearly crop production typical of the study period (Figure 2), where crop production is given by the multiplication of crop actual yield and harvested area. At the global scale, the histograms of wheat and rice are skewed toward the right with tailing off after 5000 m^3 ton^{-1}. Both crops show a high water productivity, but wheat has a larger water consumption since its production is bigger and more widespread worldwide (the average global water consumption in the

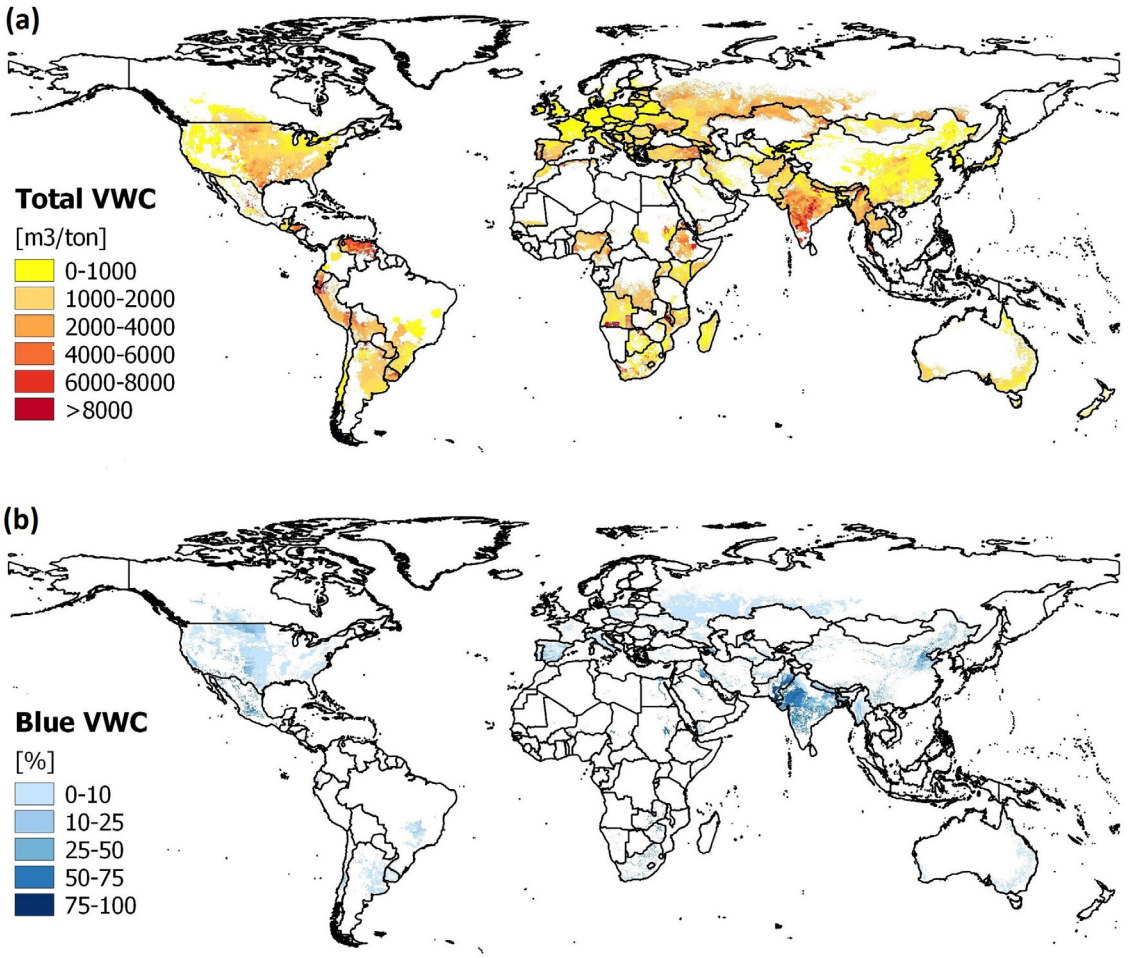

Figure 1. Spatial distribution of the virtual water content (*VWC*) of wheat in the period 1996–2005: (a) total *VWC*, expressed in m^3 ton^{-1} and (b) blue *VWC*, expressed as percentage of the total *VWC*.

considered period is about 900 Gm^3 yr^{-1}, 90% of which is green). Rice presents a lower water consumption of 870 Gm^3 yr^{-1} (85% is green). Maize exhibits a skewed right pattern with tailing off after 4000 m^3 ton^{-1}. Its production, which is the biggest one among all of these four crops, is the most efficient in terms of water consumption (830 Gm^3 yr^{-1}, 95% is green). Soybean is the most water consuming crop per tons of product; however, since it is less produced than other crops, it contributes to the smallest total water consumption (400 Gm^3 yr^{-1}, 97% is green).

Table 2. Comparison Between the *VWC* Values of Wheat, Rice, Maize, and Soybean, Evaluated in the Major Exporting Countries, From This Study and From *Hanasaki et al.* [2010]

Crop	Country	This Study	*Hanasaki et al.* [2010]
Wheat	USA	2579	1359
	Canada	1275	1800
	France	668	366
	Australia	1877	1339
	Argentina	2034	1190
Rice	Thailand	2292	1831
	Vietnam	1675	1245
	China	1087	789
Maize	USA	657	621
	Argentina	918	1041
	China	725	715
Soybean	USA	2318	1921
	Brazil	2125	2220
	Argentina	1870	2405

Figure 2a shows that Asia is the main wheat producer (3×10^8 ton yr^{-1}) and exhibits the highest virtual water variability. Europe and North America are also important contributors to the global wheat production (46 and 27% of Asian production), with a smaller *VWC* range. Asia and Europe are the most efficient regions in terms of water consumption since their production is mostly characterized by low *VWC* values:

Table 3. Comparison Between the Globally Averaged *VWC* of Wheat, Rice, Maize, and Soybean From This Study and From *Mekonnen and Hoekstra* [2011] and *Siebert and Döll* [2010]

Crop	This Study	*Mekonnen and Hoekstra* [2011]	*Siebert and Döll* [2010]
Wheat	1523	1619	1469
Rice	1607	1486	1382
Maize	933	1028	1089
Soybean	2258	2107	2406

the histograms are, in fact, skewed toward the right. However, while Europe uses nearly no blue water for wheat production (99.5% is green water), in Asia about 20% of the water footprint of wheat is contributed by blue water. North America appears to be less water efficient, because the core of its production has a higher water footprint; for example, it produces 6×10^7 ton/yr less than Europe using 3% more water. Finally, Africa, Oceania, and South America are minor wheat producers (around 7% of Asian production).

In the case of rice (Figure 2b), Asia is not only the main producer, but its production is significantly larger than that from all the other geographic areas (it accounts for 93% of the global production). Asian rice production is rather water efficient: its histogram pattern is skewed toward the right, with virtual water content mostly lower than 2000 m^3 ton^{-1}. This high efficiency is mostly due to China (which is the biggest producer), where high yields—6.5 ton ha^{-1} on average—are achieved by many varieties and hybrids with good quality and resistance to diseases and insects [*Labrada*, 2012]. Among the other geographical areas, only America and Africa give an appreciable additional contribution to world production (5.2 and 2.4% of Asian production). In particular, 40% of North America water consumption for rice production is blue, while in South America and Africa blue water contributes to the water footprint of rice only for 10 and 13%, respectively, and have an overall lower water efficiency. In relative terms, in Oceania the blue water footprint of rice is higher than in all the other continents, with more than 70% of the water consumed coming from irrigation.

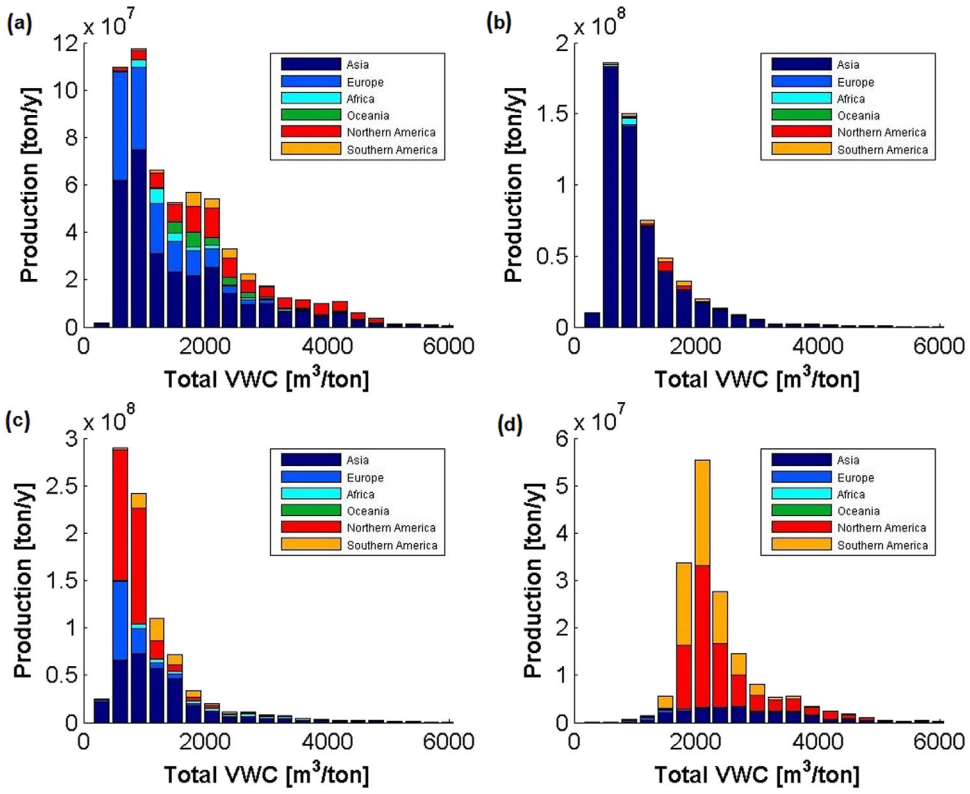

Figure 2. Distribution of the total virtual water content (*VWC*) related to yearly production: (a) wheat; (b) rice; (c) maize; and (d) soybean. In each histogram, the abscissa reports the *VWC* grouped in classes of 300 m^3 ton^{-1} width; the height of the rectangle gives the yearly production typical of the period 1996–2005 (i.e., crop actual yield multiplied by harvested area) for each class and geographical area, rectangle area indicates the volume of water used. We separate the contribution of North and South America in correspondence of Panama.

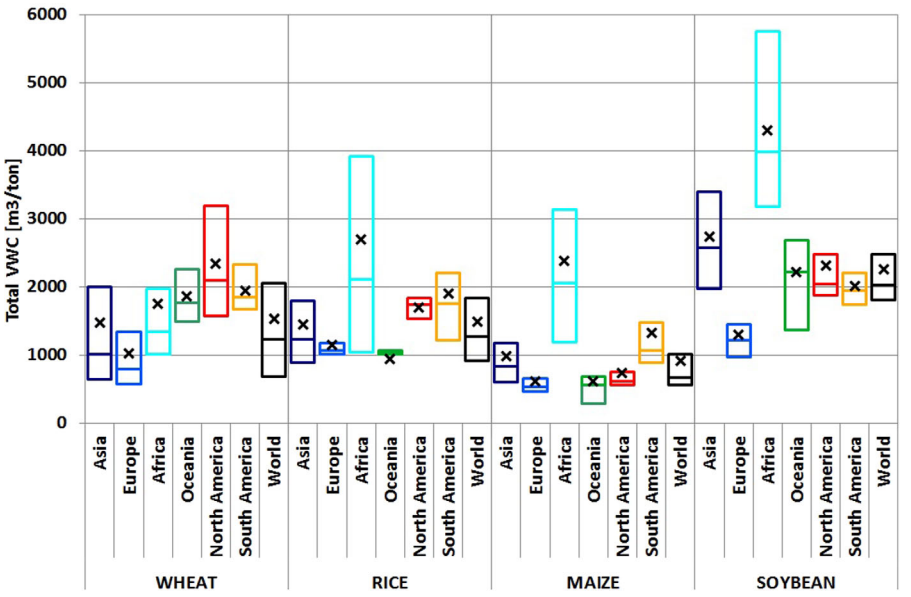

Figure 3. Boxplots and weighted means (represented by cross markers) of the *VWC* of wheat, rice, maize, and soybean aggregated by continents. Boxplots have been obtained considering *VWC* cell values in ascending order together with the relative cumulative production and quantiles have been determined in correspondence to 25, 50, 75% of total production.

Ninety percent of the global production of maize is located in Asia and America (Figure 2c), with the United States leading the water efficiency of the region with an average water footprint of 660 m^3 ton^{-1}. The *VWC* of North America shows a small spatial variability, with values generally lower than 1000 m^3 ton^{-1} and mostly contributed by green water. Conversely, Asia is characterized by a higher heterogeneity similar to the one of wheat and rice. Europe (where 15% of the global production is located) exhibits an efficiency similar to the one observed in North America both in terms of total consumed water and in terms of green contribution. The Americas are the biggest producers of soybean (Figure 2d). North and South America present similar *VWC* distributions, with a higher variability in North America. Asia is also an important producer, with an overall symmetric distribution of virtual water contents, indicating a lower water efficiency compared to other crops.

3.3. Statistical Distribution of VWC Related to Production

Boxplots in Figure 3 directly compare the crops *VWC*, grouping data at a continental scale, and highlight the associated variability as a function of production. The *VWC* values calculated for the pixels within each continent are sorted in an ascending-order vector which is then used to sort the cumulated percentage of cell production values. Quartiles are determined in correspondence to 25, 50, 75% of the cumulated production. The average values are obtained as a production weighted mean of the cell *VWC* values (i.e., cell production is used as the weight in the average).

At a global scale, maize is the crop with the lowest *VWC* value, 910 m^3 ton^{-1} on average. Except for the case of Africa, all geographic areas show a *VWC* lower than 1500 m^3 ton^{-1} for, at least, 75% of total production, or even lower than 800 m^3 ton^{-1} in Europe, Oceania, and North America. Moreover, most of the areas exhibit a relatively low spatial variability (with Europe and North America being the most homogeneous regions). On the contrary, African virtual water contents range from 1000 (e.g., Egypt, Kenya, Madagascar, and South Africa) to over 3000 m^3 ton^{-1} (e.g., Ethiopia, Nigeria, and Congo). The lowest *VWC* values are obtained in those regions where irrigation prevents the crops from water stress and yield reduction, or in those areas where high yielding genetically modified maize is planted, as in South Africa [*Shiferaw et al.*, 2011].

Rice shows an average virtual water content of 1487 m^3 ton^{-1}. As expected, its global *VWC* range is very similar to the one found for Asia (which is the biggest producer). Similarly to maize, Africa presents the largest virtual water content (2700 m^3 ton^{-1}) and the widest interquantile range (1000–4000 m^3 ton^{-1}). Europe,

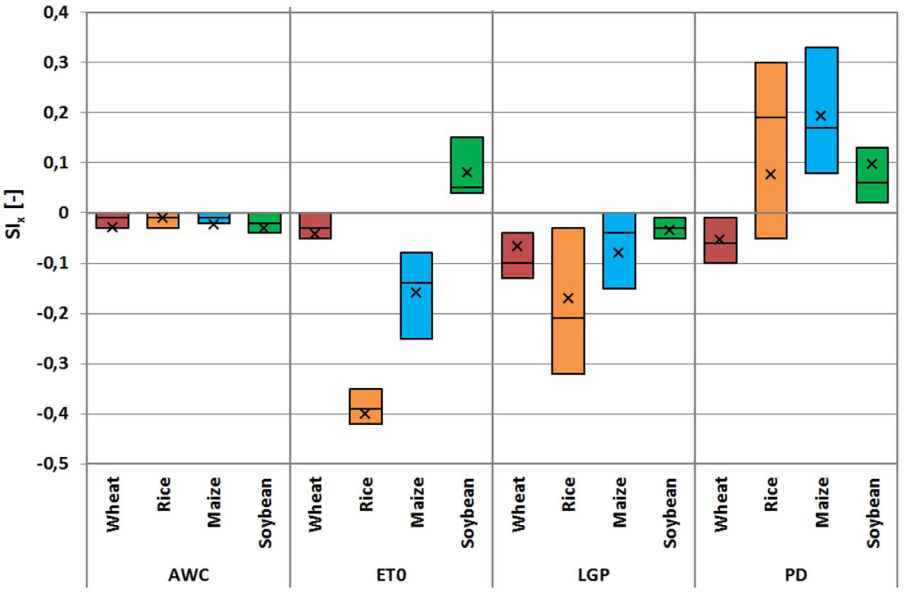

Figure 4. Boxplots and average values (represented by cross markers) of the sensitivity index (SI_x) of each parameter *x*. *AWC*: available water content, $ET_{0,m}$: reference evapotranspiration, *LGP*: length of the growing period, and *PD*: planting date.

Oceania, and North America exhibit a very low spatial variability, which is explained by their homogeneous harvested areas where little differences in yields and evapotranspiration demands can be observed.

Wheat shows an average virtual water content of 1520 m^3 ton^{-1}. In this case, all the geographical areas show a quite similar *VWC* spatial variability (as shown by the similar interquantile ranges in Figure 3): wheat is, in fact, the most widely cultivated cereal in the world with more than 220 $\times$ 10^6 ha planted annually [*Shiferaw et al*., 2013]. Thus, wheat is grown under a wide range of climatic conditions (i.e., evapotranspiration pattern), soil properties, and production methods (i.e., yield pattern) which determine the wide range of *VWC*s. The United States exhibit the highest *VWC*. African water efficiency is mostly determined by Egypt (i.e., the biggest producing country in Africa). Thanks to the fertility of the Nile Valley, Egypt can achieve wheat yields similar to those of Europe, the region where wheat production has the highest water efficiency.

Finally, soybean exhibits the highest virtual water content, 2260 m^3 ton^{-1} on global average. Such a high value is mostly due to North and South America and, to a lesser extent, Asia. All the geographical areas have an average *VWC* value shifted above 2000 m^3 ton^{-1}, except for Europe that appears to be the most water efficient region, similarly to the cases of wheat and maize. Conversely, African values are really high, with an average *VWC* value of 4250 m^3 ton^{-1}.

4. Sensitivity Analysis for the Virtual Water Content

The sensitivity analysis gives important insights into the model performance in terms of key input parameters. Positive and negative variations of the input parameters are found to produce *VWC* variations of the same magnitude, but in opposite directions. Therefore, here we provide the sensitivity indexes, SI_x for parameter *x*, only with respect to positive variations. In Figure 4, we report the average sensitivity indexes, SI_x (evaluated with equation (11)) at the global scale, boxplots quantiles are referred to production with the same approach used for the boxplots in Figure 3 (see section 3.3). In Figure 5, we report the map (at 5 $\times$ 5 arc min resolution) of the wheat *VWC* sensitivity to the *LGP* variation, SI_{LGP}. Other maps of SI_x are provided as supporting information (Figures S4–S7).

4.1. Available Water Content

The available water content (*AWC*) is the difference between the water content at field capacity and wilting point. It varies across the grid cells with values from 3.75 to 150 mm m^{-1}, depending on the soil properties.

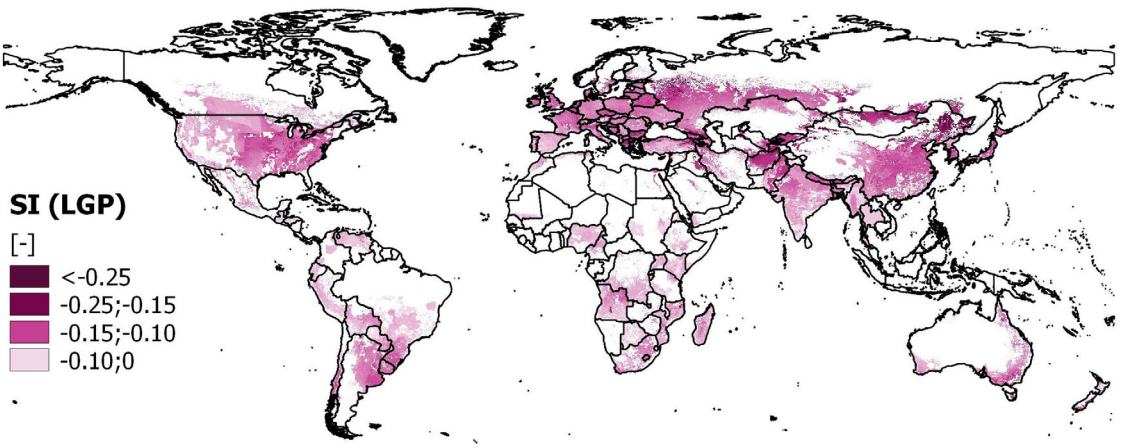

Figure 5. The sensitivity index of the *VWC* of wheat to the length of the growing period (*LGP*). The length of the growing period is varied of 1 day.

This parameter, together with the rooting depth (R_j) and the depletion fraction (ρ), defines the readily available water content (*RAW*) that the crop can use to evapotranspire without experiencing water stress (see the equations (A2) and (A3)). Thus, *RAW* is the water content defining incipient stomata closure and transpiration reduction ($k_s < 1$, see equation (A1)). In the sensitivity analysis, the available water content is varied by ± 1 mm m^{-1}. The variation in *AWC* produces a variation of *RAW*, and thus a shift of the initial stomata closure to different water contents. For example, an increment of *AWC* implies that crop becomes water stressed later during the growth season, resulting in a larger actual evapotranspiration ($ET_{a,LGP}$). In detail, green evapotranspiration increases while blue evapotranspiration decreases. The reduction of the blue component is explained by the lower irrigation requirement, since the condition $D_{mo,j} \leq RAW_j$ (see Appendix A) is satisfied for a longer period; as a consequence the green component increases.

All crops (see Figure 4) exhibit negative sensitivity indexes (SI_{AWC}); a negative SI_{AWC} means that an increment of the *AWC* produces a reduction of the crop *VWC* due to the higher achieved yields (see equation (12)) through the higher evapotranspiration rates. The virtual water content of rice is the least sensitive to *AWC* variations. Rice water stress is, in fact, controlled by irrigation (75% of the total harvested area is, in fact, irrigated), thus the positive effect of increasing the available water content is limited and the increase of *ET* and *Y* is merely appreciable. For wheat, maize, and soybean the water content is more substantially influenced by the *AWC* and precipitation. In fact, these crops are less frequently irrigated (<30% of the total harvested area), and thus they are more influenced by the soil water conditions.

4.2. Reference Evapotranspiration

Monthly reference evapotranspiration, $ET_{0,m}$, is cell-specific and represents the daily average evapotranspiration during a given month. The linear interpolation of $ET_{0,m}$ gives the daily temporal evolution of the reference evapotranspiration, $ET_{0,j}$, during the year, with j being the day of the year. Planting and harvesting date, which are crop and cell-specific, define the range of j. The $ET_{0,j}$ value, multiplied by the daily crop coefficient ($k_{c,j}$), determines the daily evapotranspiration demand, which directly influences the crop virtual water content.

In the sensitivity analysis, $ET_{0,m}$ is varied by ± 0.01 mm d^{-1} (with respect to the baseline values given by *New et al*. [2002]) and the new daily $ET_{0,j}$ is determined. For the sake of simplicity, we discuss here only the changes in virtual water content associated to positive variations of $ET_{0,m}$.

Depending on the soil water content and irrigation conditions, the new *ET* demand can be totally or partially satisfied. In the irrigated production, the new water requirement can be partly met by irrigation, with larger evapotranspirations of blue water. In the rainfed production, the ability of the new evapotranspiration demand to be met depends on the water available from precipitation. Higher evapotranspiration demand can take better advantage of precipitation (i.e., higher evapotranspiration of green water), if available, thereby limiting runoff and water losses. The *VWC* variations have opposite directions for different crops as

shown by the sensitivity indexes in Figure 4. Soybean exhibits a positive sensitivity index around 0.08, indicating that a positive variation of $ET_{0,m}$ increases the crop water footprint. A possible reason lies in the yield response factor, K_y—that relates Y reductions to ET reductions in equation (12)—which is equal to 0.85. According to *Doorenbos and Kassam* [1979], $K_y < 1$ implies that the crop exhibits a less-than-proportional increase in the yield with increased actual evapotranspiration. Supporting information Figure S4 shows the $SI_{ET_{0,m}}$ spatial variability with a high-resolution map. Considering the biggest producers, the United States (located in the temperate belt) exhibits lower sensitivities to $ET_{0,m}$ variations than Brazil and India (located in the tropical zone), where the $SI_{ET_{0,m}}$ reaches values around 0.15. Wheat, rice, and maize show negative sensitivity indexes; for these crops, an increased evapotranspiration reduces the virtual water content due to increased yields. These crops, in fact, are very sensitive to water surplus, as shown by their yield response factor which is equal or higher than 1, indicating that the yield increases more-than-proportionally when ET increases. The VWC of rice is the most sensitive to evapotranspiration variations, as shown by a $SI_{ET_{0,m}}$ value of −0.4 on average. The sensitivity index of rice is quite heterogeneous at subnational scale (refer to supporting information Figure S5), with values between −0.10 and −0.60 (e.g., South Sudan, Ethiopia, and Tanzania).

4.3. Length of the Growing Season

The length of the growing period, LGP, defined by the planting and the harvesting date, is used to calculate the length of the four growth stages (l_{st}) defining the shape of the piecewise crop coefficient curve.

The sensitivity of VWC to LGP is evaluated by varying LGP of ±1 day. The variation makes a stage of the growing season 1 day longer or shorter than the nominal value, while the other three stages are shifted of 1 day (i.e., the crop is harvested later or earlier), maintaining their initial length. Such translation changes the daily crop water requirement because k_c is differently associated with daily ET_0 values, impacting the virtual water content.

Wheat exhibits a sensitivity index of −0.05 on average (see Figure 4). The negative values of SI_{LGP} indicate that the virtual water content has decreased due to the increased yields. In fact, a 1 day longer growing season implies a higher ET demand, which can be partially or totally met by precipitation or irrigation, depending on the cultivation conditions. The spatial variability of the wheat SI_{LGP} (Figure 5) ranges between the tropical zone where the sensitivity indexes are around −0.05 and the temperate belt and the subtropical (summer rainfall) zones where these indexes reach values around −0.25. In these areas, in fact, the yield increases more than elsewhere (about 1.5–2.5% with respect to the baseline value) because the increased ET demand is totally met by irrigation in the Nile Basin, in the North of India, and in the North-East of China, and by precipitation in Belgium, Netherlands, Northern Italy, and Mongolia. Rice, maize, and soybean show negative sensitivity indexes of −0.18, −0.09, and −0.03, respectively.

4.4. Crop Planting Date

Crop planting dates were taken from *Portmann et al*. [2010]. This database provides the months when the growing season starts and ends, making a distinction between rainfed and irrigated production. The intermediate day of the month is taken as the planting date. Varying the planting date (±1 day), with constant length of the growing period, implies a rigid translation of the growing season to higher or lower daily reference evapotranspirations. Therefore, the SI_{PD} depends on the month of the year in which the crop is planted and on the temporal evolution of ET_0 during the growing season, and it may also include negative values. On global average, rice, maize, and soybean exhibit positive sensitivity indexes: 0.08, 0.18, and 0.1, respectively, with cells showing strong spatial heterogeneity, especially for rice harvested areas where some cell show negative sensitivity indexes (see Figure 4). For these crops, a 1 day shift in the growing period increases the virtual water content. Rice, maize, and soybean are, in fact, spring or summer crops, thus a positive variation of the planting date implies a shift of the growing period to lower reference evapotranspiration periods, and thus lower crop water requirement and virtual water content. The map in supporting information Figure S6 better specifies the spatial variability shown by the boxplots; for example, focusing on the main rice producers (e.g., China, India, and Vietnam), the SI_{PD} values vary from −1 to 1 depending on the water conditions of each harvested area. Southern India shows a SI_{PD} value of −1 indicating an attenuation of the crop water footprint due to the increased yield of 0.5%; Northern India exhibits a positive sensitivity index around 0.8 due to a decreased yield, which reaches −2% in those cells under rainfed conditions. The map in supporting information Figure S7 shows the SI_{PD} values of maize and help to localize the positive SI_{PD} values; the temperate zone is positively sensitive to planting date changes due to yield

reductions caused by *ET* attenuations. The SI_{PD} value presents a significant within-countries spatial variability, which is particularly evident in Brazil, India, and China. The sensitivity index of wheat *VWC* goes in the opposite direction with an average value of −0.05. This means that delaying the planting date of wheat (which is mostly a winter crop) helps to reduce its water footprint. However, in some wheat producing areas (e.g., located in the tropical belt) the behavior is the opposite one, with positive SI_{PD} values.

5. Conclusions

The high-resolution maps of the virtual water content (*VWC*) of the main cultivated crops have been obtained using recently high-resolution data and accounting for multicropping practices. The *VWC* values differ substantially among crops and across production regions, exhibiting strong spatial heterogeneity even at the subnational scale. The spatial heterogeneity in the *VWC* is mainly driven by the yield patterns with a correlation coefficient higher than 0.7 for all the crops. This suggests that the crop *VWC* is influenced by agricultural practices more than climatic conditions. This is an important result, especially in terms of indicating a strategy toward virtual water content reduction; *Rockström and Barron* [2007], for example, have shown that there is a great opportunity to improve water productivity (and thus reduce *VWC*) through the improvement of yield levels within the available water balance in rainfed agriculture, without requiring additional blue water resources. Furthermore, considering the logarithmic relationship existing between *VWC* and yield, the largest water productivity gains can be achieved in the two main hot spot regions of the world in terms of poverty and water scarcity, i.e., sub-Saharan Africa and South Asia, where the *VWC* estimates are generally above the global average due to the low crop yields.

Aggregate analyses at the continental scale provide a global view of the *VWC* value in relation to crop production. From the histograms in Figure 2 and from the boxplots in Figure 3, it is clear that wheat, rice, and maize are characterized by a higher water productivity (and thus lower virtual water content) than soybean, due to their higher yields. However, soybean yield, as well as the production area, is expected to increase with the help of genetic resources which may provide the solution needed to overcome abiotic and biotic constraints [*Hartman et al*., 2011]. The results of the aggregate analysis also show the global consumptive water use of the four grains, which is about 3000 $km^3\ yr^{-1}$ in the period from 1996 to 2005. Green water contributed to 90% of the global consumptive water use in the crop growing periods; this high proportion of green water is partly due to the dominance of rainfed agriculture. In addition, in irrigated lands, green water contributed to 25–80% of the total consumptive water use as also shown, at the grid-cell scale, by the maps of blue *VWC*. In fact, only in some regions and countries (e.g., Egypt, Pakistan, and Saudi Arabia) crop production depends primarily on blue water. The important role of green water in crop production highlights the need for a better management of this water resource.

Most notably, to our knowledge this is the first study assessing, at the global scale, the sensitivity of the *VWC* estimates to the model-inputs. The results of the sensitivity analysis show that wheat is the most sensitive crop to the length of the growing period, rice to the reference evapotranspiration, maize and soybean to the crop planting date. Virtual water content shows different sensitivity to input parameters not only among crops, but also across the harvested areas of the world, even at the subnational scale. These results may inform future efforts aiming at the refinement of data used in the assessment of agricultural water requirements and lend themselves to the identification of the parameters that farmers and land managers can modify to effectively reduce the water cost for crop production. Virtual water content estimates and sensitivity studies will need to be extended toward other crops and other water using processes, at different spatiotemporal scales, to have a complete picture of this effective tool to tackle water and food security.

Appendix A: Computation of the Water Stress Coefficient, k_s

Allen et al. [1998] defined the daily water stress coefficient as

$$k_{s,j} = \frac{TAW_j - D_{mo,j}}{TAW_j - RAW_j}, \tag{A1}$$

where TAW_j (mm) is the total available water content in the root zone, RAW_j (mm) is the readily available water content, and $D_{mo,j}$ (mm) is the root zone depletion in the morning (i.e., the water shortage relative to field capacity).

TAW_j depends on the available soil water content per meter depth, AWC (mm m^{-1}), and on the daily rooting depth, R_j (m), according to

$$TAW_j = AWC \cdot R_j \quad (\text{mm}). \tag{A2}$$

Grid-based data on AWC, at 30 × 30 arc sec resolution, were taken from *FAO/IIASA/ISRIC/ISSCAS/JRC* [2012] and converted to 5 × 5 arc min through an average. The rooting depth, R_j, is given by *Allen et al.* [1998]. R_j generally increases during the first two growing stages up to a maximum value (dependent on crop type and irrigation conditions) and then it remains constant until the harvest day.

RAW_j is the water that crops can use for evapotranspiration before water stress and stomata closure begin. It is given by

$$RAW_j = \rho \cdot TAW_j \quad (\text{mm}). \tag{A3}$$

RAW_j depends on the average fraction of TAW, ρ, that can be depleted from the root zone before moisture stress occurs, and it is different among species. We assumed ρ to be constant during the growing season (ρ values are given by *Allen et al.* [1998]). The different values of TAW and RAW in rainfed and irrigated production are due to the different rooting depth (which is deeper in rainfed production). Root zone depletion is recorded in the morning, $D_{mo,j}$, depending on daily precipitation, irrigation, and crop evapotranspiration.

In rainfed production (R), the root zone depletion in the morning, $D_{mo,j}$, is equal to the one recorded at the end of the previous day ($D_{ev,(j-1)}$), minus the daily precipitation value, P_j,

$$D_{mo,j} = D_{ev,(j-1)} - P_j \quad \left(\frac{\text{mm}}{\text{d}}\right). \tag{A4}$$

Daily precipitation is obtained equally distributing the monthly climatic precipitation along the growing period with daily frequency. For sake of simplicity, all months are assumed 30 days long. Monthly climatic precipitation are available in the literature at 10 × 10 arc min resolution [*New et al.*, 2002]; we convert this data to 5 × 5 arc min grid cells as done in section 2.1 for reference evapotranspiration. $D_{mo,j}$ is equal to 0 on the planting day. In the evening $D_{mo,j}$ increases because of crop evapotranspiration, as

$$ET_{a,j} = k_{c,j} \cdot ET_{0,j} \cdot \frac{TAW_j - D_{mo,j}}{TAW_j - RAW_j}, \tag{A5}$$

$$D_{ev,j} = D_{mo,j} + ET_{a,j} \quad \left(\frac{\text{mm}}{\text{d}}\right). \tag{A6}$$

We did not consider water lost by deep percolation, and the capillary rise was assumed equal to zero, whereas water excess (leading to negative values of $D_{mo,j}$) were cut off at zero and the exceeding precipitation was assumed to be lost as surface runoff. In rainfed conditions, the water volume evapotranspired by the crop during the growth period is totally green, $ET_{g,LGP} = ET_{a,LGP}$.

In irrigated production (I), irrigation is required when rainfall is insufficient to compensate for the water loss by evapotranspiration. By calculating the soil water balance of the root zone on a daily basis, the timing and depth of irrigation can be planned. To avoid crop water stress, irrigation water should be applied before or at the moment when the readily available soil water is depleted ($D_{mo,j} \geq RAW_j$). $D_{mo,j}$ is given by equation (A4) and RAW_j is given by equation (A3). To avoid deep percolation losses that may leach relevant nutrients out of the root zone, the net irrigation depth should be smaller than or equal to the root zone depletion ($I_j \leq D_{mo,j}$). The daily net volume of irrigation is determined with the assumption that the crop fully evapotranspires without suffering from water stress throughout the day; the water volume is given by the following relationship:

$$I_j = D_{mo,j} - RAW_j + k_{c,j} \cdot ET_0 \quad (\text{mm}). \tag{A7}$$

Irrigation brings the root zone depletion in the morning down to the readily available water content (i.e., $D_{mo,j} = RAW_j$), and supplies the crop with the water required to satisfy its evapotranspiration demand throughout the day (namely $k_{c,j} \cdot ET_0$). In the evening, the root zone depletion is given by

$$D_{ev,j} = D_{mo,j} + ET_{a,j} - I_j \quad \left(\frac{\text{mm}}{\text{d}}\right), \tag{A8}$$

where $ET_{a,j}$ is given by equation (5) with $k_{s,j}=1$. $ET_{a,j}$ is the water volume evapotranspired by the crop during the day; the water volume consists of green and/or blue water. The blue water, $ET_{b,j}$, corresponds to the irrigation water given to the crop (namely, $ET_{b,j}=I_j$); the green water, $ET_{g,j}$, is evaluated as the difference between the total and the blue water evapotranspiration.

Appendix B: The Normalization of Input Parameters Required in the Sensitivity Analysis

The normalization of the parameter variation required by the sensitivity index defined in equation (11) is different for the four parameters analyzed. In detail, the variation of the available water content (*AWC*) is normalized with respect to the baseline value; the variation of the planting date (*PD*) is normalized with respect to 360 days (namely the number of days of a year considering each month 30 days long); the variation of the reference evapotranspiration ($ET_{0,m}$) and the length of the growing period (*LGP*) are normalized as follow. After changing their baseline values of a fixed quantity (0.01 mm d^{-1} and 1 day, respectively), the new virtual water content of the rainfed and the irrigated production, as well as the relative variations ΔVWC, are evaluated. The normalized sensitivity index are separately determined for rainfed and irrigated conditions, with specific values of x_{ref}, that are (i) the ratio between the total reference evapotranspiration over the growing period and *LGP* for $ET_{0,m}$, and (ii) the length of the growing season typical of rainfed and irrigated conditions for *LGP*. Finally, the overall sensitivity indexes of these parameters, $SI_{ET_{0,m}}$ and SI_{LGP}, are calculated as the weighted mean of the rainfed and irrigated sensitivity indexes, using the harvested area given by *Portmann et al*. [2010] as the weights.

Acknowledgments

The authors wish to thank funding support provided by the Italian Ministry of Education, University and Research (MIUR) through the project "The global virtual-water network: social, economic, and environmental implications" (FIRB-RBFR12BA3Y). Data and results are available upon request. The anonymous reviewers are greatly acknowledged for their valuable suggestions.

References

Allan, J. A. (2003), Virtual water-the water, food, and trade nexus. Useful concept or misleading metaphor?, *Water Int.*, *28*(1), 106–113.

Allen, R. G., L. Pereira, D. Raes, and M. Smith (1998), Crop evapotranspiration: Guidelines for computing crop water requirements, *FAO Irrig. Drain. Pap.*, *56*, 26–40.

Antonelli, M., and M. Sartori (2015), Unfolding the potential of the virtual water concept. What is still under debate?, *Environ. Sci. Policy.*, doi:10.2139/ssrn.2533435.

Bocchiola, D., E. Nana, and A. Soncini (2013), Impact of climate change scenarios on crop yield and water footprint of maize in the Po valley of Italy, *Agric. Water Manage.*, *116*, 50–61.

Bouman, B., E. Humphreys, T. Tuong, and R. Barker (2007), Rice and water, *Adv. Agron.*, *92*, 187–237.

Carr, J. A., P. D'Odorico, F. Laio, and L. Ridolfi (2013), Recent history and geography of virtual water trade, *PloS One*, *8*(2), e55825.

Chapagain, A., and A. Hoekstra (2011), The blue, green and grey water footprint of rice from production and consumption perspectives, *Ecol. Econ.*, *70*(4), 749–758.

Chapagain, A. K., and A. Y. Hoekstra (2004), *WaterFootprints of Nations, Value Water Res. Rep. Ser.*, UNESCO-IHE Inst. for Water Educ., Delft, Netherlands. [Available at http://doc.utwente.nl/77203/.]

D'Odorico, P., J. A. Carr, F. Laio, L. Ridolfi, and S. Vandoni (2014), Feeding humanity through global food trade, *Earth Future*, *2*(9), 458–469.

Doorenbos, J., and A. H. Kassam (1979), Yield response to water, *FAO Irrig. Drain. Pap.*, *33*, 257.

Dudgeon, D., et al. (2006), Freshwater biodiversity: Importance, threats, status and conservation challenges, *Biol. Rev.*, *81*(2), 163–182.

Falkenmark, M., and J. Rockström (2004), *Balancing Water for Humans and Nature: The New Approach in Ecohydrology*, Earthscan, U. K.

FAO (2011), *The State of the World's Land and Water Resources for Food and Agriculture: Managing Systems at Risk*, Rome.

FAO/IIASA/ISRIC/ISSCAS/JRC (2012), *Harmonized World Soil Database (version 1.2)*. Rome.

FAO (2014), *Geonetwork*, Rome. [Available at http://www.fao.org/geonetwork/srv/en/main.home.]

Fedoroff, N., et al. (2010), Radically rethinking agriculture for the 21st century, *Science*, *327*(5967), 833–834.

Gleick, P. H. (2000), A look at twenty-first century water resources development, *Water Int.*, *25*(1), 127–138.

Godfray, H. C. J., et al. (2010), Food security: The challenge of feeding 9 billion people, *Science*, *327*(5967), 812–818.

Hanasaki, N., T. Inuzuka, S. Kanae, and T. Oki (2010), An estimation of global virtual water flow and sources of water withdrawal for major crops and livestock products using a global hydrological model, *J. Hydrol.*, *384*(3), 232–244.

Hanjra, M. A., and M. E. Qureshi (2010), Global water crisis and future food security in an era of climate change, *Food Policy*, *35*(5), 365–377.

Hartman, G. L., E. D. West, and T. K. Herman (2011), Crops that feed the World 2. Soybean—Worldwide production, use, and constraints caused by pathogens and pests, *Food Security*, *3*(1), 5–17.

Hoekstra, A. Y., and A. K. Chapagain (2011), *Globalization of Water: Sharing the Planet's Freshwater Resources*, John Wiley, Hoboken, N. J.

Hoekstra, A. Y., and P. Hung (2002), Virtual water trade, in *A Quantification of Virtual Water Flows Between Nations in Relation to International Crop Trade, Value Water Res. Rep. Ser.*, 11, 166 pp., UNESCO-IHE Inst. for Water Educ., Delft, Netherlands. [Available at http://waterfootprint.org/Reports/Report11.pdf.]

Konar, M., C. Dalin, S. Suweis, N. Hanasaki, A. Rinaldo, and I. Rodriguez-Iturbe (2011), Water for food: The global virtual water trade network, *Water Resour. Res.*, *47*, W05520, doi:10.1029/2010WR010307.

Kummu, M., H. De Moel, M. Porkka, S. Siebert, O. Varis, and P. Ward (2012), Lost food, wasted resources: Global food supply chain losses and their impacts on freshwater, cropland, and fertiliser use, *Sci. Total Environ.*, *438*, 477–489.

Labrada, R. (2012), The need for improved weed management in rice, paper presented at 20th Session of the International Rice Commission, Agric. and Consumer Prot., Bangkok, 23–26 Jul.

Liu, J., and H. Yang (2010), Spatially explicit assessment of global consumptive water uses in cropland: Green and blue water, *J. Hydrol.*, *384*(3), 187–197.

Lobell, D. B., K. G. Cassman, and C. B. Field (2009), Crop yield gaps: Their importance, magnitudes, and causes, *Annu. Rev. Environ. Resour.*, *34*(1), 179.

Mekonnen, M. M., and A. Y. Hoekstra (2011), The green, blue and grey water footprint of crops and derived crop products, *Hydrol. Earth Syst. Sci.*, *15*(5), 1577–1600.
Monfreda, C., N. Ramankutty, and J. A. Foley (2008), Farming the planet: 2. Geographic distribution of crop areas, yields, physiological types, and net primary production in the year 2000, *Global Biogeochem. Cycles*, *22*, GB1022, doi:10.1029/2007GB002947.
Mueller, N. D., J. S. Gerber, M. Johnston, D. K. Ray, N. Ramankutty, and J. A. Foley (2012), Closing yield gaps through nutrient and water management, *Nature*, *490*(7419), 254–257.
New, M., D. Lister, M. Hulme, and I. Makin (2002), A high-resolution data set of surface climate over global land areas, *Clim. Res.*, *21*(1), 1–25.
Portmann, F. T., S. Siebert, and P. Döll (2010), Mirca2000global monthly irrigated and rainfed crop areas around the year 2000: A new high-resolution data set for agricultural and hydrological modeling, *Global Biogeochem. Cycles*, *24*, GB1011, doi:10.1029/2008GB003435.
Rockström, J., and J. Barron (2007), Water productivity in rainfed systems: Overview of challenges and analysis of opportunities in water scarcity prone savannahs, *Irrig. Sci.*, *25*(3), 299–311.
Rost, S., D. Gerten, A. Bondeau, W. Lucht, J. Rohwer, and S. Schaphoff (2008), Agricultural green and blue water consumption and its influence on the global water system, *Water Resour. Res.*, *44*, W09405, doi:10.1029/2007WR006331.
Seekell, D., P. DOdorico, and M. Pace (2011), Virtual water transfers unlikely to redress inequality in global water use, *Environ. Res. Lett.*, *6*(2), 024017.
Shiferaw, B., B. M. Prasanna, J. Hellin, and M. Bänziger (2011), Crops that feed the World 6. Past successes and future challenges to the role played by maize in global food security, *Food Security*, *3*(3), 307–327.
Shiferaw, B., M. Smale, H.-J. Braun, E. Duveiller, M. Reynolds, and G. Muricho (2013), Crops that feed the World 10. Past successes and future challenges to the role played by wheat in global food security, *Food Security*, *5*(3), 291–317.
Siebert, S., and P. Döll (2010), Quantifying blue and green virtual water contents in global crop production as well as potential production losses without irrigation, *J. Hydrol.*, *384*(3), 198–217.
Tamea, S., J. Carr, F. Laio, and L. Ridolfi (2014), Drivers of the virtual water trade, *Water Resour. Res.*, *50*, 17–28, doi:10.1002/2013WR014707.
Tilman, D., C. Balzer, J. Hill, and B. L. Befort (2011), Global food demand and the sustainable intensification of agriculture, *Proc. Natl. Acad. Sci. U. S. A.*, *108*(50), 20,260–20,264.
United Nations, Department of Economic and Social Affairs, Population Division (2013), World population prospects: The 2012 revision, Highlights and advance tables, *Working Pap. ESA/P/WP.228*.
Vanham, D., M. Mekonnen, and A. Hoekstra (2013), The water footprint of the EU for different diets, *Ecol. Indicators*, *32*, 1–8.
Wada, Y., L. P. van Beek, C. M. van Kempen, J. W. Reckman, S. Vasak, and M. F. Bierkens (2010), Global depletion of groundwater resources, *Geophys. Res. Lett.*, *37*, L20402, doi:10.1029/2010GL044571.
Wichelns, D. (2004), The policy relevance of virtual water can be enhanced by considering comparative advantages, *Agric. Water Manage.*, *66*(1), 49–63.
Wickham, T., and V. Singh (1978), Water movement through wet soils, in *Soils and Rice*, pp. 337–358, Int. Rice Res. Inst., Los Baños, Philippines.
Zhuo, L., M. Mekonnen, and A. Hoekstra (2014), Sensitivity and uncertainty in crop water footprint accounting: A case study for the yellow river basin, *Hydrol. Earth Syst. Sci. Discuss.*, *11*(1), 135–167.